

Variability in the subcellular distribution of ion channels increases neuronal diversity

Zoltan Nusser

Laboratory of Cellular Neurophysiology, Institute of Experimental Medicine, Hungarian Academy of Sciences, 1083 Budapest, Hungary

The exact location of an ion channel on the axo-somato-dendritic surface of a nerve cell crucially affects its functional impact. Recent high-resolution immunolocalization experiments examining the distribution of GABA and glutamate receptors, voltage-gated potassium and sodium channels and hyperpolarization-activated mixed cation (HCN) channels clearly demonstrate the lack of simple rules concerning their subcellular distribution. For example, the density of HCN1 subunits in pyramidal cells increases 60-fold from soma to distal dendrites but is uniform over the somato-dendritic surface of olfactory bulb external tufted cells and is highest in the axon of cortical and cerebellar basket cells. Such findings highlight the necessity of determining the precise subcellular location and density of each ion channel in every cell type. Here, I suggest that variations in the subcellular distribution of ion channels are previously unrecognized means of increasing neuronal diversity and, thus, the computational power of the brain.

Introduction

Distinct neuronal networks, constituted by different types of neurons with unique synaptic connectivity patterns, perform widely different functions such as the generation of intrinsic rhythms for controlling breathing, discrimination between two odor molecules or wavelengths of light, execution of movements or laying down memories for a lifetime. It is no wonder that understanding neuronal diversity and network connectivity has become a main focus of experimental neuroscience. Already at the turn of the 20th century the ingenious work of Camillo Golgi [1], Santiago Ramon y Cajal [2] and Rafael Lorent de No [3] began to reveal the morphological diversity of nerve cells and their specific synaptic connectivity. Later on, after the introduction of modern molecular and electrophysiological methods, the functional heterogeneity of nerve cells also became evident. We have only superficial knowledge about how the morphological diversity of nerve cells is achieved, but it is now a general belief that the variation in the intrinsic electrical properties of neurons is the consequence of the expression of distinct sets of ion channels. Understanding diverse electrical properties of nerve cells was one of the incentives driving the tremendous efforts of the past two decades to identify the molecular diversity of ion

channels and their expression patterns in the central nervous system CNS (e.g. the Allen Brain Atlas).

For simple spherical cells, the density of a cell-surface protein in the plasma membrane is usually controlled at the level of mRNA expression. Thus, experiments using single-cell RT-PCR or *in situ* hybridization histochemistry provide useful information from which meaningful functional predictions can be made. However, nerve cells are morphologically the most complex cells of our body, bearing extensive and elaborate dendritic and axonal arbors, the total length of which can exceed several centimeters and contain thousands of branches. The future of newly synthesized cell-surface proteins is much less certain in such a complex cell; they could either uniformly occupy the entire plasma membrane or could be selectively targeted to certain subcellular compartments such as axon terminals, nodes of Ranvier, axon initial segments (AISs), somata, proximal or distal dendritic shafts or dendritic spines. An additional degree of complexity arises from the potential of having different channel densities at these subcellular compartments (i.e. increased or decreased densities from proximal to distal dendrites). Thus, simply knowing the expression of an ion channel mRNA in nerve cells is not sufficient for generating meaningful predictions of function; instead, the precise subcellular distribution of the protein and its density in each subcellular compartment must be determined. This was recently recognized by many investigators who, according to their individual technical expertise, employed patch-clamp electrophysiology, Ca²⁺ imaging or immunohistochemistry to investigate the subcellular distribution of voltage- and ligand-gated ion channels. The results of these efforts have been the subject of many excellent reviews focusing on different aspects of ion channel distribution, surface targeting, regulation and plasticity [4–14]. An emerging view regarding the subcellular location of ion channels is that each ion channel has its own unique subcellular distribution pattern (e.g. N-methyl-D-aspartic acid [NMDA] receptors: synaptic; HCN1: dendritic; K_v2.1: perisomatic; K_v1.1: axonal; Na_v1.1: AIS; Na_v1.6: AIS and nodes of Ranvier). An erroneous notion that arose from these studies is that the subcellular distribution of a protein needs to be determined only once in a ‘model’ cell and the result will be readily applicable for all nerve cells. Here, I aim to highlight results of recent high-resolution immunolocalization experiments demonstrating that the precise subcellular

Corresponding author: Nusser, Z. (nusser@koki.hu)

location of ligand- and voltage-gated ion channels varies among neuron types. Consequently, ion channel distribution is cell-type specific and likely to help produce the remarkable neuronal diversity present in the CNS.

Cell-type- and synaptic-input-dependent subcellular distribution of AMPA receptors

α -Amino-3-hydroxyl-5-methyl-4-isoxazole-propionate (AMPA)-type glutamate receptors (AMPA receptors) are ubiquitously present in every nerve cell. They are assumed to be concentrated in postsynaptic specializations of glutamatergic synapses and are present at a low density in the extrasynaptic plasma membrane. This general view is probably the consequence of many studies examining the subcellular location of AMPA receptor subunits in hippocampal CA1 pyramidal cells (PCs) [15–20]. The question arises whether this pattern is true for all nerve cells or whether alternative distribution patterns also exist. In other words, in what other ways could AMPA receptors be distributed on the neuronal surface? There is an almost endless number of potential permutations of molecularly distinct AMPA receptors, each at variable densities, in each subcellular compartment (i.e. axon, soma, dendrite, synaptic, extrasynaptic). In the next paragraphs I will highlight a few, well-documented examples of presynaptic input- and postsynaptic cell-type-dependent expression patterns of AMPA receptors.

Although ionotropic glutamate receptors have been assumed to be concentrated in glutamatergic synaptic junctions, there are many examples showing a lack of their enrichment in all synaptic junctions. Electron microscopic immunogold localization experiments have revealed that the AMPA receptor content of Schaffer collateral synapses on CA1 PCs varies to such an extent that some synapses have several hundred whereas some others might not even have any AMPA receptors [15,18–20]. Is this large synapse-to-synapse variation, with some ‘silent’ synapses, thus the general feature of AMPA receptor distribution? No. The presence of AMPA receptors in all glutamatergic synapses has been demonstrated in cerebellar granule [21], Purkinje and stellate/basket cells [22]. Of note, using quantitative postembedding immunogold localization of AMPA receptors in cerebellar granule cells, DiGregorio *et al.* [21] concluded that these receptors are only located synaptically, given that no detectable level of extrasynaptic receptors was observed. This result is consistent with the lack of AMPA-receptor-mediated currents in recordings from outside-out patches excised from the extrasynaptic somatic membranes of granule cells [23].

As mentioned earlier, synaptic AMPA receptor number is highly variable in Schaffer-collateral–CA1-PC synapses. A similar quantitative distribution pattern was found in commissural/associational fiber synapses on CA3 PCs. However, when mossy fiber synapses, which connect granule cells of the dentate gyrus to CA3 PCs, were examined, a much higher number and density of AMPA receptors and a much lower synapse-to-synapse variability was found [15,18]. An almost identical result was obtained in cerebellar Purkinje cells. Parallel fiber synapses contain a low density and highly variable number of AMPA receptors, whereas climbing fiber synapses on the same cells are

strongly immunopositive for AMPA receptors with low synapse-to-synapse variation [22]. Thus, the number, density and variability of synaptic AMPA receptors depend on the cell type and the synaptic input. In another study [24], the AMPA receptor GluR2 subunit was found at both parallel and auditory fiber synapses in fusiform cells of the dorsal cochlear nucleus with approximately the same density, whereas the GluR4 subunit was only detectable at auditory synapses. These results demonstrate that neurons can show input-specific differences in AMPA receptor number, density, variability and subunit composition.

The subsynaptic distributions of AMPA receptors are also variable. Masugi-Tokita and Shigemoto [4,22] have used freeze-fracture replica labeling of AMPA receptor subunits in the cerebellar cortex and found that immunogold particles are evenly distributed in parallel-fiber–interneuron and climbing-fiber–Purkinje-cell synapses. By contrast, the same subunits form small microclusters in parallel-fiber–Purkinje-cell synapses. Similar subsynaptic microclusters have been previously reported for γ -aminobutyric acid (GABA)_A receptors [25].

Robust cell-type-specific differences in the presynaptic distribution of AMPA receptors have also been demonstrated. Fujiyama *et al.* [26] revealed presynaptic GluR1, GluR2/3 and GluR4 subunit-containing receptors in cortico-striatal axon terminals, whereas cortico-cortical axon terminals lack all of these subunits. Thalamo-striatal terminals also contain presynaptic GluR1 and GluR2/3, but are devoid of the GluR4 subunit, demonstrating that both the presynaptic cell type (thalamic versus cortical axon onto striatal cells) and the postsynaptic target cell (cortical versus striatal cells for the cortical inputs) influence the expression of presynaptic AMPA receptors. In this study, immunogold particles were concentrated in the presynaptic active zone, but cell-type-specific heterogeneities might also occur at the level of axonal subcompartments (e.g. active zone, nonsynaptic bouton versus preterminal axon), as has been shown for some voltage-gated ion channels and metabotropic glutamate receptors.

There might be many other neuron-type-specific features of the subcellular distribution of AMPA receptors. A recent study demonstrated that the density of AMPA receptors in perforated synapses increases in CA1 PCs from proximal to distal stratum radiatum [20]. Such a distance-dependent distribution has not been examined in any other cell type with electronmicroscopic immunogold localization, but inferring from functional experiments I suspect that distance-dependent scaling of synaptic AMPA receptor number is not usually true for all nerve cells but is a specific feature found only in certain cell types. For example, Williams and Stuart [27] have examined AMPA-receptor-mediated excitatory postsynaptic potentials in neocortical layer 5 PC apical dendrites and concluded that synaptic AMPA receptor conductance is distance independent. This is in contrast to the finding of Magee and colleagues [28] in CA1 PCs where AMPA-receptor-mediated synaptic conductance increases as a function of distance in the stratum radiatum.

I also hypothesize that the extrasynaptic density of AMPA receptors might vary among dendritic regions

innervated by distinct synaptic inputs in such a way that highly plastic inputs are surrounded by a higher density of extrasynaptic receptors, whereas the extrasynaptic AMPA receptor density is low around non-plastic synapses. It is likely that future high-resolution localization studies will reveal many other previously unexpected cell-type-specific features of the subcellular distribution of AMPA receptors.

In summary, glutamatergic inputs to CA1 PCs act through synapses that show high synapse-to-synapse variability in their AMPA receptor content. By contrast, all glutamatergic synapses in cerebellar stellate/basket cells contain a high and invariable density of AMPA receptors. In cerebellar Purkinje and CA3 PCs the density and variability of AMPA receptors is input dependent, whereas it is the subunit composition in fusiform cells of the cochlear nucleus that shows synaptic input dependence. The extrasynaptic AMPA receptor expression is also cell-type dependent; the density of receptors is substantial in hippocampal PCs, low in Purkinje cells, yet they are undetectable in cerebellar granule cells [4,21,22]. Cell-type-dependent variation in the subcellular distribution of NMDA and GABA_A receptors has also been described [29–31], indicating that this is a general rule for all ligand-gated ion channels rather than a specific feature of AMPA receptors.

Cell-type-dependent axo-somato-dendritic distribution of hyperpolarization-activated mixed cation channels

The hyperpolarization-activated mixed cation current (I_h) is mediated by HCN channels composed of homo- or heteromultimeric assemblies of four subunits (HCN1 to HCN4). This current has essential roles in the pacemaker activity of the heart and influences the resting membrane potential, rhythmic activity and temporal summation of synaptic inputs in central neurons. HCN subunits have distinct expression patterns in the CNS; HCN2 has a widespread distribution, whereas HCN1, HCN3 and HCN4 are primarily present in the cortex, hypothalamus and thalamus, respectively [32,33]. The subcellular distribution of I_h was first studied by Magee [34]; using somatic and dendritic-cell-attached recordings in CA1 PCs, he found an increase in current density as he patched further out from the soma along the main apical dendrite. Using light and electron microscopic immunohistochemistry, Lorincz *et al.* [35] provided direct evidence for an increased density of HCN1 subunit from the soma to proximal and distal apical dendrites of CA1 PCs. A very similar somato-dendritic distribution pattern was found in subicular (Figure 1a) and neocortical layer 5 PCs, in agreement with the results of functional studies [36,37], invoking the notion that this distribution pattern might be valid for all HCN1 subunit-expressing cells. However, further investigations using high-resolution immunohistochemical methods in many brain regions revealed that the distance-dependent increase in dendritic HCN channel density is not a general rule for all nerve cells. For example, HCN1 is present rather uniformly in the somatic and dendritic plasma membranes of external tufted and periglomerular cells of the main olfactory bulb [38] (Figure 1b). An even more surprising finding is that HCN1 is not present at all in the somato-dendritic plasma membrane of hippocampal basket cells but has a high density in their

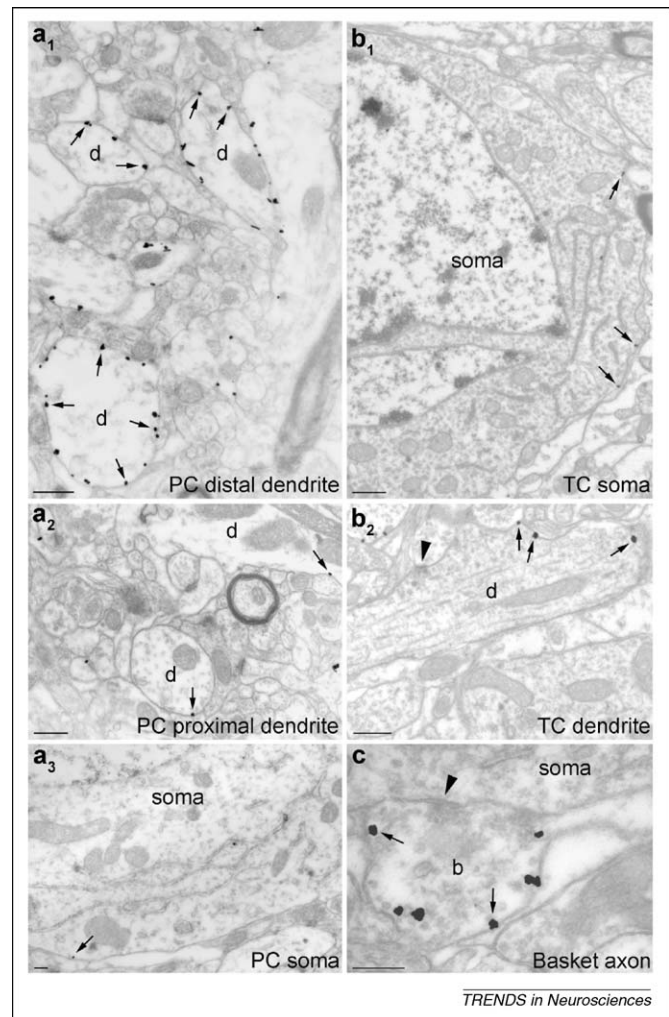


Figure 1. Electron microscopic immunogold demonstration of the cell-type-specific differential subcellular distribution of HCN1. (**a**₁–**a**₃) Pre-embedding immunogold localization of HCN1 in distal (**a**₁), proximal (**a**₂) dendrites and somata (**a**₃) of subicular pyramidal cells (PCs). Note the very high density of immunogold particles (arrows) along the plasma membranes of distal dendrites (labeled as d) and the contrasting infrequent labeling of proximal dendritic shafts and somatic plasma membranes. (**b**₁,**b**₂) The density of HCN1 immunolabeling (arrows) in the somatic plasma membrane (soma in **b**₁) of external tufted cells of the main olfactory bulb is similar to that found in their dendrites (labeled as d in **b**₂). Note that the tufted cell dendrite (labeled as d) establishes an asymmetrical synaptic junction (arrowhead) with a small diameter presumed periglomerular cell dendrite. (**c**) A high density of gold particles (arrows) is shown on a basket cell axon terminal (labeled as b) establishing a symmetrical synaptic junction (arrowhead) with a hippocampal pyramidal cell soma (soma). Scale bars: (a) 0.4 μm, (b) 0.5 μm, (c) 0.2 μm. Images **a**₁–**a**₃ are from Ref. [35].

axon terminals and preterminal axons [32,39] (Figure 1c). The finding of Lujan *et al.* [40] adds another twist to this story; HCN1 immunolabeling in cerebellar basket cells was found throughout the axo-somato-dendritic surface with slightly higher levels in axon terminals. These results reveal at least four distinct subcellular distribution patterns for the HCN1 subunit (Figure 2). It is important to note that the subcellular distribution and density of HCN channels also show variability within a single cell type. Recently, Garden *et al.* [41] elegantly demonstrated differences in I_h densities in entorhinal cortical layer 2 stellate cells; the density of I_h depended on the dorso-ventral location of the cells and paralleled the gradient in the size of their grid fields. Currently, no immunolocalization data exists on such within-cell-type cell-to-cell variability on ion

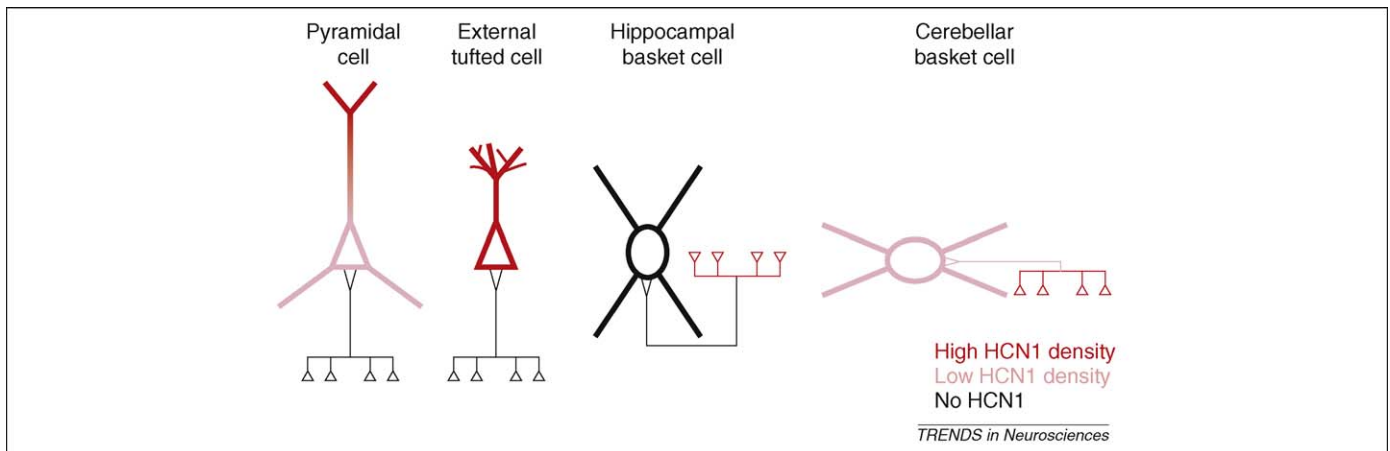


Figure 2. Schematic illustration of the diversity of the subcellular distribution of HCN1 subunit in distinct types of neuron. Subcellular distribution of the HCN1 subunit in four types of nerve cells. Red indicates high levels, pink indicates low levels and black indicates the lack of the HCN1 subunit in the plasma membrane. In cortical layer 5 and hippocampal PCs, the density of the HCN1 subunit increases from the soma to proximal and distal apical dendrites. In external tufted cells of the main olfactory bulb, HCN1 has a uniform somato-dendritic density. In hippocampal basket cells, HCN1 is primarily localized to the axon terminals and preterminal axons, whereas in cerebellar basket cells it is present at a low density in the somato-dendritic plasma membrane and at a slightly higher density in axon terminals.

channel distributions and densities, but such variations are expected to increase neuronal diversity in an activity-dependent manner [42–44].

Is it only the HCN1 subunit that has such an intricate subcellular distribution, or does a similar complexity characterize the distribution of the other subunits? In hippocampal and neocortical PCs, the HCN2 subunit has an almost identical subcellular distribution to that of HCN1 (i.e. distance-dependent increase in the dendrites), whereas it is present in axons in the main olfactory bulb, medial habenular nucleus and hippocampal basket cells [32]. Although HCN2 is confined to preterminal axons and axon terminals in hippocampal basket cells, it is located in myelinated axons in the medial habenula [32]. It is easy to envisage the functional consequences of somato-dendritic versus axonal location of I_h , but it is much more challenging to understand why certain dendrites contain a uniform density whereas some others have an increasing density of I_h [45]. Similarly, it is not easy to predict the role of HCN channels in myelinated axons or to design experiments in which the functional consequences of the location in preterminal axons versus axon terminals are tested. Nevertheless, I am confident that future studies using *in vitro* imaging and electrophysiology on state-of-the-art genetically modified animals will find solutions to these puzzles.

The subcellular distribution of HCN channels is probably the best studied among voltage-gated ion channels in the CNS. Although there are many voltage-gated channels for which we have little or zero information about their subcellular distribution, I suspect similar complexities in their subcellular distributions to those demonstrated for glutamate receptors and HCN channels. In the next paragraphs, I provide a brief summary of recent experiments examining the subcellular distribution of $K_v4.2$, $Na_v1.1$ and $Na_v1.6$ subunits.

Uniform versus clustered subcellular distribution of A-type K^+ channels

Voltage-gated K^+ channels comprise the largest family of voltage-gated ion channels with ~ 40 different subunits,

forming many dozens of functionally distinct channel assemblies [46]. Although the K_v4 subfamily has only three members ($K_v4.1$, $K_v4.2$ and $K_v4.3$), it has received special attention owing to the wealth of information on the functional roles of transient, or A-type, K^+ currents (I_A), which are primarily mediated by these subunits [10,13,47]. In a very elegant study, Hoffman *et al.* [48] examined I_A in CA1 PCs with somatic and dendritic patch-clamp recordings and found an increased current density from proximal to distal apical dendrites. This uneven distribution of I_A regulates dendritic action-potential initiation, attenuates dendritic-spike back propagation and reduces distal excitatory postsynaptic responses. Because the inhomogeneous density of I_A is very similar to that found for I_h in the same cells, and because the density of HCN1 and HCN2 proteins shows a dramatic increase in CA1 PC apical dendrites, a similar increase in the density of K_v4 subunits was expected. Because CA1 PCs express only the $K_v4.2$ subunit from the K_v4 subfamily, several investigators addressed this issue using light microscopic immunohistochemistry with $K_v4.2$ subunit-specific antibodies. Surprisingly, a rather uniform distribution of the $K_v4.2$ subunit in CA1 PC apical dendrites was inferred from the homogenous labeling of the stratum radiatum of the CA1 area [49,50]. However, such a homogenous labeling as observed at the light microscopy level does not exclude the possibility that these channels have a nonuniform subcellular distribution on CA1 PC apical dendrites. Namely, a high density of the $K_v4.2$ subunit in apical oblique dendrites could mask a lower, but proximo-distally increasing, channel density in apical dendritic shafts.

In CA1 PCs no obvious clusters of immunoreactivity for the $K_v4.2$ subunit were observed. However, in many other cell types, the cell-surface distribution of $K_v4.2$ subunit is rather inhomogeneous, with many strongly immunopositive clusters. For example, in cortical PCs, Burkhalter *et al.* [51] found clustering of the $K_v4.2$ subunit in postsynaptic specialization of GABAergic, but not glutamatergic, synapses. A similar synaptic clustering of this subunit was reported by Jinno *et al.* [49] in parasubicular PCs. In our laboratory, we have also examined the subcellular

distribution of the $K_v4.2$ subunit in a variety of nerve cells and consistently found clustered cell-surface distributions. For example, in some cerebellar stellate/basket cells, the $K_v4.2$ subunit co-clustered with the $K_v4.3$ subunit in membrane specializations between climbing fiber terminals and stellate/basket cell somata and dendrites [52]. A very prominent clustering was found in nerve cells of the main olfactory bulb [53]. These $K_v4.2$ subunit enrichments were observed in membranes specializations, which did not show any morphological or molecular feature of known chemical or electrical synapses. Such K^+ -channel-rich junctions were observed in the main olfactory bulb between adjacent granule cells, between adjacent mitral cells, between mitral and granule cells, between external tufted and periglomerular cells, and also among adjacent nerve cells of the medial habenular nucleus. These results, taken together, again demonstrate many different $K_v4.2$ subcellular distribution patterns; in some cells they seem to be uniformly distributed without high-density clusters, whereas in the majority of cells prominent clustering occurs. These clusters seem to be either in GABAergic synaptic junctions or in the so-called K^+ -channel-rich specializations. The functional consequences of the clustered distribution of A-type K^+ channels subunits is as yet

unknown, but their participation in a novel form of inter-cellular communication [54] has been suggested [52,53].

Differential axonal distribution of voltage-gated Na^+ channels

It has been recently demonstrated that $Na_v1.1$ and $Na_v1.6$ subunits are localized differentially in retinal ganglion cell AISs. The $Na_v1.1$ subunit occupies the proximal part of the AIS, where the $Na_v1.6$ subunit is at very low density. More distally, where the $Na_v1.6$ subunit density increases, the $Na_v1.1$ subunit becomes undetectable [55]. A very similar sub-AIS segregation of these two subunits was found in neocortical and hippocampal parvalbumin positive interneurons [55–57] (Figure 3a). Again, these initial results invoke the notion that this subcellular distribution pattern might be widely true for all nerve cells. However, examining a few other cell types in different brain regions revealed that the $Na_v1.1$ subunit is not exclusively present in proximal AISs. In GABAergic basket cells of the cerebellar cortex, for example, both the proximal part of the AIS and the main axons running parallel with the Purkinje cell layer are labeled for the $Na_v1.1$ subunit, with the latter being strongly immunopositive [56,57] (Figure 3c). Furthermore, Ogiwara *et al.* [56] found $Na_v1.1$ subunit

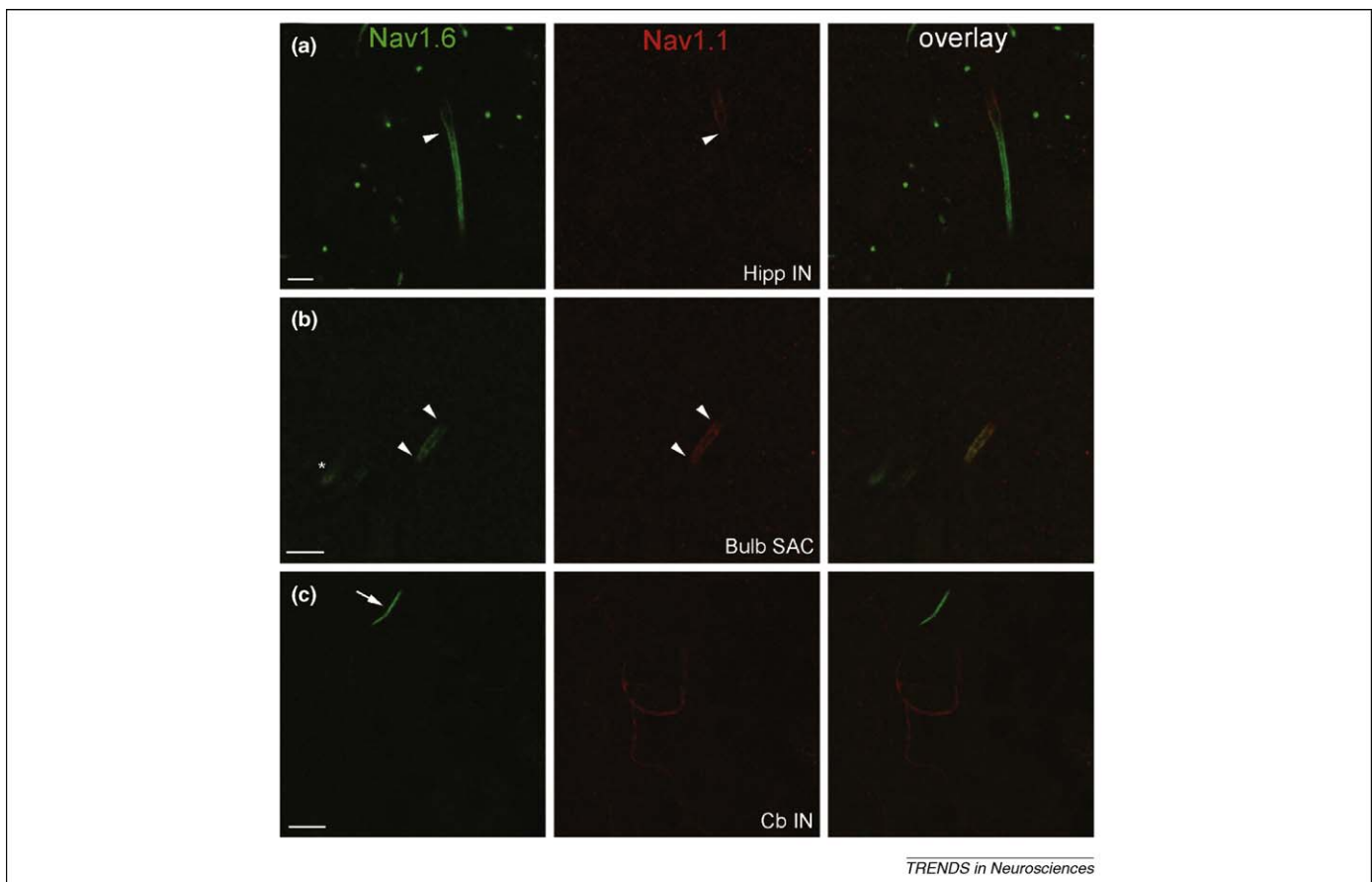


Figure 3. Differential sub-axonal distribution of $Na_v1.1$ in three cell types. (a) Double immunofluorescent labeling for the $Na_v1.1$ and $Na_v1.6$ subunits in the hippocampal CA3c area. The $Na_v1.1$ and $Na_v1.6$ subunits are segregated in an AIS of a GABAergic interneuron. Arrowhead indicates where immunoreactivity for $Na_v1.1$ subunit becomes undetectable. Maximum intensity projection of eight confocal images taken at $0.5 \mu\text{m}$ axial separation. (b) In the external plexiform layer of the main olfactory bulb, both the $Na_v1.1$ and $Na_v1.6$ subunits occupy the entire length (between the two arrowheads) of the AIS of a short-axon cell. Part of the AIS of a tufted cell is also visible within these confocal sections (asterisk), which is immunopositive only for the $Na_v1.6$ subunit. Maximum intensity projection of two confocal images taken at $0.5 \mu\text{m}$ axial separation. (c) Immunoreactivity for the $Na_v1.6$ subunit is confined to the AIS of basket cells in the proximal *stratum moleculare* of the cerebellar cortex (arrow), whereas the $Na_v1.1$ subunit is present within the main axons of these cells. Maximum intensity projection of three confocal images taken at $1 \mu\text{m}$ axial separation. Scale bars: (a,b) $5 \mu\text{m}$, (c) $10 \mu\text{m}$. Abbreviations: Cb IN, cerebellar interneuron; Hipp IN, hippocampal interneuron; Bulb SAC, olfactory bulb short-axon cell.

immunoreactivity in nodes of Ranvier in the deep cerebellar nuclei and in the corpus callosum. In the rat main olfactory bulb, the $\text{Na}_v1.1$ subunit is confined to the proximal part of the AIS of deep short-axon cells of the infratramital layers, similarly to that found in cortical interneurons. However, it is present throughout the entire length of the AIS of short-axon cells of the external plexiform layer (Figure 3b) [57], demonstrating at least four distinct $\text{Na}_v1.1$ subunit distribution patterns.

In addition to the $\text{Na}_v1.1$ subunit, the subcellular distribution of the $\text{Na}_v1.6$ subunit has also been studied. This is a ubiquitously expressed ion channel subunit, apparently present in almost all nerve cells. The subcellular distribution of this protein is qualitatively very similar in all cell types studied; it is found in AISs and nodes of Ranvier without detectable levels in the somata, dendrites, preterminal axons and axon terminals [55,57–61]. However, there are apparent quantitative differences among the AISs. For example, the AISs of middle tufted cells of the olfactory bulb external plexiform layer are much more intensely labeled for the $\text{Na}_v1.6$ subunit than the neighboring AISs of short axon cells [57]. To quantify the exact differences in the density of $\text{Na}_v1.6$ subunit in different subcellular compartments, highly sensitive, quantitative, high-resolution immunolocalization experiments will need to be carried out [4,22].

Differences in the subcellular distribution of ion channels is a way of increasing neuronal diversity

In simple spherical cells, ion channels in the plasma membrane are either present or not; therefore, the number of permutations producing distinct functional ‘phenotypes’ is simply the function of the number of available genes. Two different ion channels enable the creation of four different cell types (Figure 4a). For nerve cells with complex morphology, the same number of functionally different cell types can be achieved if each ion channel is always located in the same subcellular compartment. For example, if channel ‘red’ is either not expressed or present in the somato-dendritic plasma membrane, whereas channel ‘green’ is either not expressed or located in the AIS and nodes of Ranvier, still only four different cell types can be created (Figure 4b). Needless to say that from hundreds of ion channel genes, using even this simple combinatorial scheme the potential number of permutations is already very large. However, if both ‘red’ and ‘green’ channels could be located in axon terminals, AIS or somato-dendritically, either alone or in any combination of these, the number of different permutations becomes 64. Figure 4c illustrates only a small fraction of these possibilities. In reality there are many more functionally relevant subcellular compartments than the three mentioned here (e.g. in PCs: axon terminals, preterminal axons, myelinated axons, nodes of Ranvier, AIS, somata, proximal and distal apical dendritic shafts and spines, and basal dendritic shafts and spines). Furthermore, in this example I have not taken into account differences in the density of the ion channels in different compartments. The 12 aforementioned subcellular compartments combined with two different channel densities (low and high) and only two ion channel subtypes would result in tens of thousands of functional ‘phenotypes’. If all

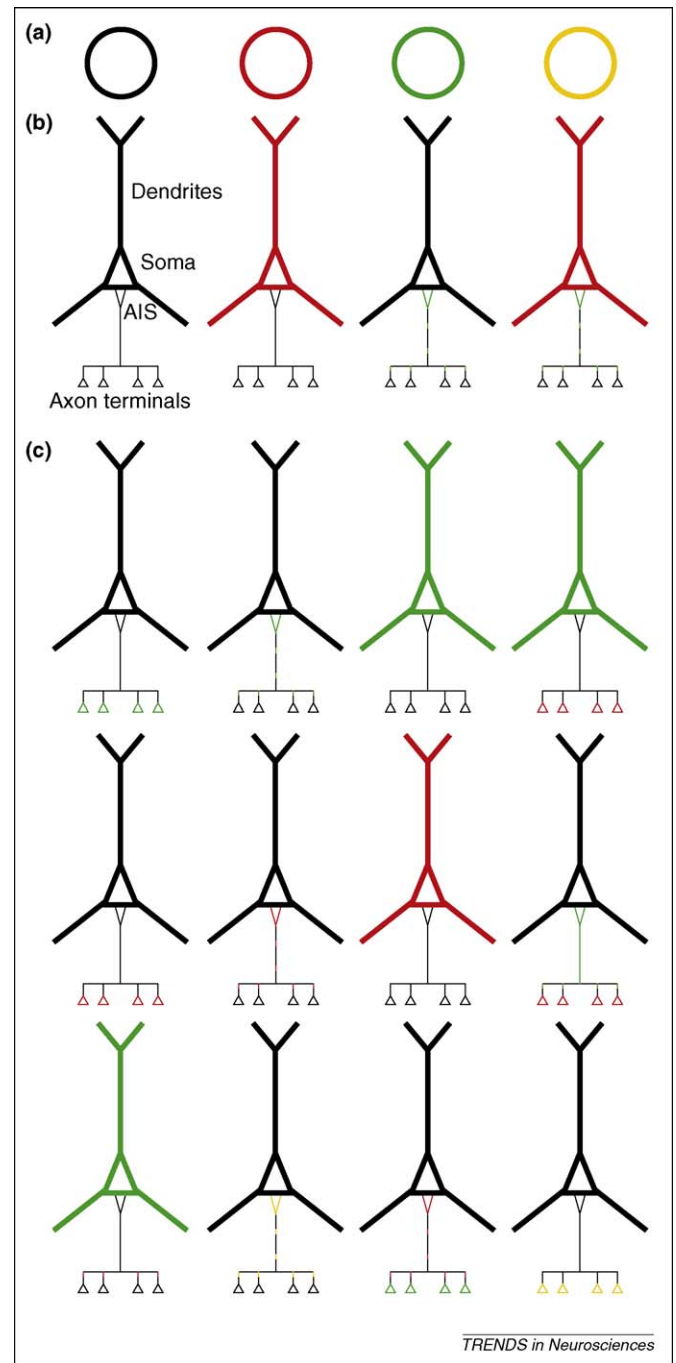


Figure 4. Schematic illustration of increased neuronal diversity by differential subcellular distribution of ion channels. (a) In simple spherical cells and using two ion channels (red and green), four different phenotypes can be created: black, red only, green only, and red and green (shown as yellow). (b) In nerve cells with complex morphology, if each ion channel is always located in the same subcellular compartment (red: soma and dendrite; green: AIS and nodes of Ranvier) the number of different phenotypes is four. (c) However, if each ion channel can be located in any of the subcellular compartments, the total number of different cell types is 64, only 12 of which are shown in this panel. Black color indicates plasma membrane without ion channels.

known ion channel subunits are taken into account, the total number of permutations by far exceeds the total number of nerve cells in the whole brain. I do not suggest that every subunit is present in every possible subcellular compartment in many distinct densities, but my aim is to highlight the great potential of increasing neuronal diversity in this way.

Ionotropic GABA_A receptors are probably the champions among ion channels as far as genetic diversity is concerned. The family contains 18 different subunits forming many dozens of heteropentameric ion channel assemblies, which have very different regional, cellular and subcellular distribution patterns. By contrast, there are only two metabotropic GABA_B receptor genes, the function of which requires dimer formation, resulting in only a single GABA_B receptor subtype in the entire body. The differential subcellular targeting of this receptor is the only means of fulfilling such widely different functional roles as regulating transmitter release or providing slow dendritic inhibition. The question arises as to why, during evolution, certain functional requirements have been reached by generating multiple protein isoforms (e.g. GABA_A receptors), whereas other requirements were fulfilled by targeting an existing protein to different subcellular compartments (e.g. GABA_B receptors). Why not achieve everything through increasing molecular diversity? I cannot provide a definite answer to these questions, but I suggest that the combinatorial potentials of these two ways (genetic diversity and altering the subcellular distribution of a single molecule) provided the flexibility essential to generate a system that is robust enough to withstand myriad unexpected perturbations and plastic enough to adapt to ever increasing functional demands. As a result of this, a very large number of functionally distinct cell types, generated in many different ways [62], reside in our CNS, the appropriate wiring of which generates the astonishing human brain.

Acknowledgements

I thank Mark Eyre, Mark Farrant and Andrea Lorincz for their comments on the manuscript. Z.N. is the recipient of a Wellcome Trust Project grant (www.wellcome.ac.uk), a European Young Investigator Award (www.esf.org/eurym) and a European Commission Integrated Project grant (EUSynapse project; LSHM-CT-2005-019055; ec.europa.eu). The support from these foundations is greatly acknowledged.

References

- Golgi, C. (1898) On the structure of nerve cells. 1898. *J. Microsc.* 155, 3–7
- Ramon y Cajal, S. (1911) *Histologie du systeme nerveux de l'homme et des vertebres*. Maloine
- Lorente de No, R. (1934) Studies on the structure of the cerebral cortex. II. Continuation of the study of the ammonic system. *J. Psychol. Neurol.* 46, 113–177
- Masugi-Tokita, M. and Shigemoto, R. (2007) High-resolution quantitative visualization of glutamate and GABA receptors at central synapses. *Curr. Opin. Neurobiol.* 17, 387–393
- Lai, H.C. and Jan, L.Y. (2006) The distribution and targeting of neuronal voltage-gated ion channels. *Nat. Rev. Neurosci.* 7, 548–562
- Williams, S.R. and Stuart, G.J. (2003) Role of dendritic synapse location in the control of action potential output. *Trends Neurosci.* 26, 147–154
- Craig, A.M. and Boudin, H. (2001) Molecular heterogeneity of central synapses: afferent and target regulation. *Nat. Neurosci.* 4, 569–578
- Nusser, Z. (2000) AMPA and NMDA receptors: similarities and differences in their synaptic distribution. *Curr. Opin. Neurobiol.* 10, 337–341
- Ottersen, O.P. and Landsend, A.S. (1997) Organization of glutamate receptors at the synapse. *Eur. J. Neurosci.* 9, 2219–2224
- Magee, J.C. and Johnston, D. (2005) Plasticity of dendritic function. *Curr. Opin. Neurobiol.* 15, 334–342
- Migliore, M. and Shepherd, G.M. (2002) Emerging rules for the distribution of active dendritic conductances. *Nat. Rev. Neurosci.* 3, 362–370
- Trimmer, J.S. and Rhodes, K.J. (2004) Localization of voltage-gated ion channels in mammalian brain. *Annu. Rev. Physiol.* 66, 477–519
- Johnston, D. *et al.* (2003) Active dendrites, potassium channels and synaptic plasticity. *Philos. Trans. R. Soc. Lond. B Biol. Sci.* 358, 667–674
- Spruston, N. (2008) Pyramidal neurons: dendritic structure and synaptic integration. *Nat. Rev. Neurosci.* 9, 206–221
- Takumi, Y. *et al.* (1999) Different modes of expression of AMPA and NMDA receptors in hippocampal synapses. *Nat. Neurosci.* 2, 618–624
- Craig, A.M. *et al.* (1993) The distribution of glutamate receptors in cultured rat hippocampal neurons: postsynaptic clustering of AMPA-selective subunits. *Neuron* 10, 1055–1068
- Baude, A. *et al.* (1995) High-resolution immunogold localization of AMPA type glutamate receptor subunits at synaptic and non-synaptic sites in rat hippocampus. *Neuroscience* 69, 1031–1055
- Nusser, Z. *et al.* (1998) Cell type and pathway dependence of synaptic AMPA receptor number and variability in the hippocampus. *Neuron* 21, 545–559
- Petralia, R.S. *et al.* (1999) Selective acquisition of AMPA receptors over postnatal development suggests a molecular basis for silent synapses. *Nat. Neurosci.* 2, 31–36
- Nicholson, D.A. *et al.* (2006) Distance-dependent differences in synapse number and AMPA receptor expression in hippocampal CA1 pyramidal neurons. *Neuron* 50, 431–442
- DiGregorio, D.A. *et al.* (2002) Spillover of glutamate onto synaptic AMPA receptors enhances fast transmission at a cerebellar synapse. *Neuron* 35, 521–533
- Masugi-Tokita, M. *et al.* (2007) Number and density of AMPA receptors in individual synapses in the rat cerebellum as revealed by SDS-digested freeze-fracture replica labeling. *J. Neurosci.* 27, 2135–2144
- Silver, R.A. *et al.* (1996) Deactivation and desensitization of non-NMDA receptors in patches and the time course of EPSCs in rat cerebellar granule cells. *J. Physiol.* 493, 167–173
- Rubio, M.E. and Wenthold, R.J. (1997) Glutamate receptors are selectively targeted to postsynaptic sites in neurons. *Neuron* 18, 939–950
- Nusser, Z. *et al.* (1998) Increased number of synaptic GABA_A receptors underlies potentiation at hippocampal inhibitory synapses. *Nature* 395, 172–177
- Fujiyama, F. *et al.* (2004) Presynaptic localization of an AMPA-type glutamate receptor in corticostriatal and thalamostriatal axon terminals. *Eur. J. Neurosci.* 20, 3322–3330
- Williams, S.R. and Stuart, G.J. (2002) Dependence of EPSP efficacy on synapse location in neocortical pyramidal neurons. *Science* 295, 1907–1910
- Magee, J.C. and Cook, E.P. (2000) Somatic EPSP amplitude is independent of synapse location in hippocampal pyramidal neurons. *Nat. Neurosci.* 3, 895–903
- Watanabe, M. *et al.* (1998) Selective scarcity of NMDA receptor channel subunits in the stratum lucidum (mossy fibre-recipient layer) of the mouse hippocampal CA3 subfield. *Eur. J. Neurosci.* 10, 478–487
- Fritschy, J.-M. *et al.* (1998) Synapse-specific localization of NMDA and GABA_A receptor subunits revealed by antigen-retrieval immunohistochemistry. *J. Comp. Neurol.* 390, 194–210
- Nusser, Z. *et al.* (1996) Differential synaptic localization of two major γ -aminobutyric acid type A receptor α subunits on hippocampal pyramidal cells. *Proc. Natl. Acad. Sci. U. S. A.* 93, 11939–11944
- Notomi, T. and Shigemoto, R. (2004) Immunohistochemical localization of I_h channel subunits, HCN1–4, in the rat brain. *J. Comp. Neurol.* 471, 241–276
- Santoro, B. *et al.* (2000) Molecular and functional heterogeneity of hyperpolarization-activated pacemaker channels in the mouse CNS. *J. Neurosci.* 20, 5264–5275
- Magee, J.C. (1998) Dendritic hyperpolarization-activated currents modify the integrative properties of hippocampal CA1 pyramidal neurons. *J. Neurosci.* 18, 7613–7624
- Lorincz, A. *et al.* (2002) Polarized and compartment-dependent distribution of HCN1 in pyramidal cell dendrites. *Nat. Neurosci.* 5, 1185–1193

- 36 Williams, S.R. and Stuart, G.J. (2000) Site independence of EPSP time course is mediated by dendritic I_h in neocortical pyramidal neurons. *J. Neurophysiol.* 83, 3177–3182
- 37 Berger, T. *et al.* (2001) High I_h channel density in the distal apical dendrite of layer V pyramidal cells increases bidirectional attenuation of EPSPs. *J. Neurophysiol.* 85, 855–868
- 38 Holderith, N.B. *et al.* (2003) Cell type-dependent expression of HCN1 in the main olfactory bulb. *Eur. J. Neurosci.* 18, 344–354
- 39 Santoro, B. *et al.* (1997) Interactive cloning with the SH3 domain of N-src identifies a new brain specific ion channel protein, with homology to eag and cyclic nucleotide-gated channels. *Proc. Natl. Acad. Sci. U. S. A.* 94, 14815–14820
- 40 Lujan, R. *et al.* (2005) Preferential localization of the hyperpolarization-activated cyclic nucleotide-gated cation channel subunit HCN1 in basket cell terminals of the rat cerebellum. *Eur. J. Neurosci.* 21, 2073–2082
- 41 Garden, D.L. *et al.* (2008) Tuning of synaptic integration in the medial entorhinal cortex to the organization of grid cell firing fields. *Neuron* 60, 875–889
- 42 van Welie, I. *et al.* (2004) Homeostatic scaling of neuronal excitability by synaptic modulation of somatic hyperpolarization-activated I_h channels. *Proc. Natl. Acad. Sci. U. S. A.* 101, 5123–5128
- 43 Narayanan, R. and Johnston, D. (2007) Long-term potentiation in rat hippocampal neurons is accompanied by spatially widespread changes in intrinsic oscillatory dynamics and excitability. *Neuron* 56, 1061–1075
- 44 Campanac, E. *et al.* (2008) Downregulation of dendritic I_h in CA1 pyramidal neurons after LTP. *J. Neurosci.* 28, 8635–8643
- 45 Angelo, K. *et al.* (2007) Local and global effects of I_h distribution in dendrites of mammalian neurons. *J. Neurosci.* 27, 8643–8653
- 46 Gutman, G.A. *et al.* (2003) International Union of Pharmacology. XLI. Compendium of voltage-gated ion channels: potassium channels. *Pharmacol. Rev.* 55, 583–586
- 47 Birnbaum, S.G. *et al.* (2004) Structure and function of Kv4-family transient potassium channels. *Physiol. Rev.* 84, 803–833
- 48 Hoffman, D.A. *et al.* (1997) K^+ channel regulation of signal propagation in dendrites of hippocampal pyramidal neurons. *Nature* 387, 869–875
- 49 Jinno, S. *et al.* (2005) Postsynaptic and extrasynaptic localization of Kv4.2 channels in the mouse hippocampal region, with special reference to targeted clustering at gabaergic synapses. *Neuroscience* 134, 483–494
- 50 Rhodes, K.J. *et al.* (2004) KChIPs and Kv4 α subunits as integral components of A-type potassium channels in mammalian brain. *J. Neurosci.* 24, 7903–7915
- 51 Burkhalter, A. *et al.* (2006) Differential expression of I_A channel subunits Kv4.2 and Kv4.3 in mouse visual cortical neurons and synapses. *J. Neurosci.* 26, 12274–12282
- 52 Kollo, M. *et al.* (2006) Novel subcellular distribution pattern of A-type K^+ channels on neuronal surface. *J. Neurosci.* 26, 2684–2691
- 53 Kollo, M. *et al.* (2008) Unique clustering of A-type potassium channels on different cell types of the main olfactory bulb. *Eur. J. Neurosci.* 27, 1686–1699
- 54 Yarom, Y. and Spira, M.E. (1982) Extracellular potassium ions mediate specific neuronal interaction. *Science* 216, 80–82
- 55 Van Wart, A. *et al.* (2007) Polarized distribution of ion channels within microdomains of the axon initial segment. *J. Comp. Neurol.* 500, 339–352
- 56 Ogiwara, I. *et al.* (2007) $Na_v1.1$ localizes to axons of parvalbumin-positive inhibitory interneurons: a circuit basis for epileptic seizures in mice carrying an *Scn1a* gene mutation. *J. Neurosci.* 27, 5903–5914
- 57 Lorincz, A. and Nusser, Z. (2008) Cell-type-dependent molecular composition of the axon initial segment. *J. Neurosci.* 28, 14329–14340
- 58 Caldwell, J.H. *et al.* (2000) Sodium channel $Na_v1.6$ is localized at nodes of ranvier, dendrites, and synapses. *Proc. Natl. Acad. Sci. U. S. A.* 97, 5616–5620
- 59 Boiko, T. *et al.* (2001) Compact myelin dictates the differential targeting of two sodium channel isoforms in the same axon. *Neuron* 30, 91–104
- 60 Boiko, T. *et al.* (2003) Functional specialization of the axon initial segment by isoform-specific sodium channel targeting. *J. Neurosci.* 23, 2306–2313
- 61 Jenkins, S.M. and Bennett, V. (2001) Ankyrin-G coordinates assembly of the spectrin-based membrane skeleton, voltage-gated sodium channels, and L1 CAMs at Purkinje neuron initial segments. *J. Cell Biol.* 155, 739–746
- 62 Marder, E. and Goaillard, J.M. (2006) Variability, compensation and homeostasis in neuron and network function. *Nat. Rev. Neurosci.* 7, 563–574